Composition Maps in Self Assembled Alloy Quantum Dots

N. V. Medhekar, V. Hegadekatte, and V. B. Shenoy
Division of Engineering, Brown University, Providence, RI 02912
(Dated: January 4, 2008)

Nanoscale variations in composition arising from the competition between chemical mixing effects and elastic relaxation can substantially influence the electronic and optical properties of self-assembled alloy quantum dots. Using a combination of finite element and quadratic programming optimization methods, we have developed an efficient technique to compute the equilibrium composition profiles in strained quantum dots. We find that the composition profiles depend strongly on the morphological features such as the slopes and curvatures of their surfaces and presence of corners and edges as well as the ratio of the strain and chemical mixing energy densities. More generally, our approach provides a means to quantitatively model the interplay between the composition variations, temperature, strain and the shapes of small-scale lattice-mismatched structures.

PACS numbers: 68.65.Hb, 68.35.Dv, 68.55.Ag

Strain-driven self assembly in lattice-mismatched semiconductor *alloy* systems provides a versatile means to fabricate nanoscale islands which can serve as functional elements in optical, electronic and photo-voltaic circuits. The electronic structure of these nanoscale islands or 'quantum dots' is strongly influenced by the shape, elastic deformation and most importantly by their composition, thereby enabling the device properties to be controlled. Self assembled SiGe and InGaAs quantum dots have received particular attention as the former material system can be readily integrated with the well developed Si technology while the latter has been successfully applied in photovoltaic and photonic applications.

While a large body of experimental and theoretical work on the growth of quantum dots is available [1, 2], key factors that play a role in determining the variations in composition within the quantum dots remain poorly understood. A quantitative determination of the composition profiles is critical in device applications as variations in composition at the nanoscale can substantially influence the electronic properties. Although progress has been made in measuring the composition profiles within individual quantum dots with nanoscale resolution[3–8], information from these experiments can only be properly interpreted with models that can distinguish the differences between composition profiles under different growth conditions. A key question that one is generally faced with in these experiments is whether or not a measured profile is close to equilibrium.

In equilibrium, for a given size, shape and average composition of the dot, the composition profile is obtained by minimizing the total free energy that consists of the elastic energy and entropic and chemical mixing energies. The primary difficulty in obtaining composition profiles is that the shape, strain and composition are all coupled to each other. Subsequently, only calculations that adopt a number of simplifying assumptions such as small slopes of the sidewalls of the quantum dots [9] and linear extrapolation of the composition profiles from the surface to the bulk [10] are available. The approximations made in the calculations allow only for the analysis of pre-pyramid clusters with very shallow sidewalls. Monte Carlo methods have also been employed to analyze quasi-equilibrium composition profiles [11], but the long range nature of the elastic interactions makes statistical sampling of the large configuration space (required to obtain properly averaged composition maps in realistic structures) a very demanding and tedious task.

In this letter, we study equilibrium composition maps in quantum dots by employing the finite element method for rigorous treatment of elastic fields without any restrictions on their shape and an optimization scheme based on quadratic programming methods. We find that the shapes of the quantum dots play a very important role in determining the degree of alloy decomposition that can be achieved at a given temperature. The composition profiles in faceted quantum dots with steep sidewalls are found to be characteristically different from the corresponding case of shallow dots. In the former case, segregation of the larger alloy component in the tensile regions of the quantum dot leads to the formation of "cusped" composition profiles which manifest in the form of dimpled surface profiles upon selective etching of one of the alloy components (Fig. 1). Shallower islands on the other hand, are less decomposed and yield surface profiles with large etch pits. Both of these features have been observed during etching of SiGe quantum dots [4–6].

In order to guide the interpretation of composition maps measured in experiments, the degree of alloy decomposition in faceted quantum dots is presented in a phase diagram plotted in the space spanned by the orientation of their sidewalls and temperature. Based on this phase diagram, the effect of decomposition on the shape transition between quantum dots with different facet orientations is computed – alloy decomposition is found to significantly decrease the transition volumes for shape transformation. To further demonstrate the role of shape and strain on alloy decomposition at the nanoscale,

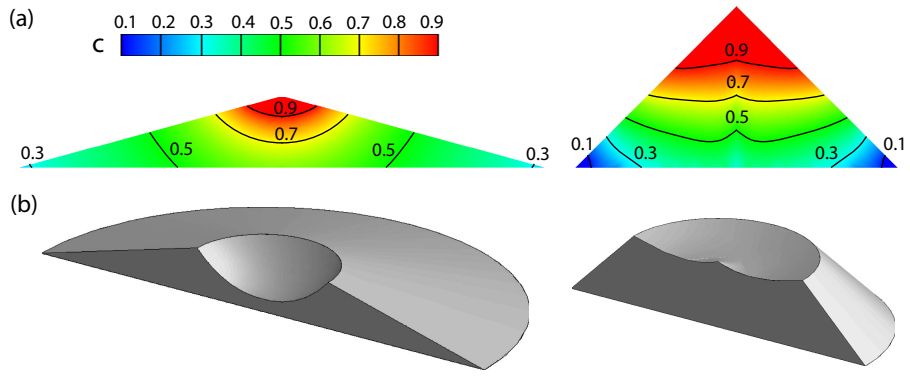

FIG. 1: (a) Composition profiles in axially symmetric quantum dots of identical size, but with shallow ($\theta = 15°$) and steep side-walls ($\theta = 30°$). The composition profiles are obtained with $F_0 = -0.2$ and $\bar{c} = 0.5$. (b) The 3D rendering of the shapes of the quantum dots in (a) upon etching with a selective chemical agent that dissolves regions of dot whose composition, c, exceeds 65%. The segregation indices (eq 4) for the steep and shallow dots are 0.177 and 0.051, respectively.

we have considered the composition profiles of dome and truncated pyramid shaped quantum dots that have been observed in SiGe [12, 13] and InGaAs [13] systems. Here we find a rich array of compositional patterns with enrichment of the larger alloy component at the corners and edges formed by the intersection of different facets.

For an AB alloy quantum dot grown epitaxially on a substrate of species A, the total free energy E of the quantum dot-substrate system can be written as $E = E_{ch} + E_{el} + E_s$, where E_{ch} is the chemical free energy of the alloy components in the quantum dot, E_{el} is the elastic strain energy due to the lattice mismatch between the quantum dot and the substrate, and E_s is the surface energy cost involved in the formation of the quantum dot. In general, the functional form of the thermodynamic mixing free energy of the alloy, which includes both enthalpic and entropic contributions, can be quite involved, although the latter contribution dominates at high temperatures, favoring complete mixing of the alloy components. In order to capture the key aspects of mixing effects, we write the chemical free energy of the alloy quantum dot as $E_{ch} = \int_{V_d} f(c)\, dV$, where V_d is the volume of the dot, $c(\mathbf{x})$ is the mole fraction (or composition) of the B-species in the alloy and the free energy density is taken to be $f(c) = \Delta F(T)\, c + F_m(T)\, c(1-c)$. Here, $\Delta F(T)$ is the free energy difference between the phases A and B and the temperature (T) dependent parameter $F_m(T)$ determines stability of the alloy to phase separation [14] – for $F_m > 0$ alloy thermodynamics favors phase separation into A and B components, while $F_m < 0$ results in complete mixing of alloy components at any composition.

The elastic energy of the quantum dot-substrate system can be written as

$$E_{el} = \frac{1}{2} \int_{V_d+V_s} C_{ijkl}(\epsilon^r_{ij} + \epsilon^0_{ij})(\epsilon^r_{kl} + \epsilon^0_{kl})\, dV\,, \qquad (1)$$

where ϵ^r_{ij} is the relaxation strain and $\epsilon^0_{ij} = \epsilon_m c(\mathbf{x})\delta_{ij}$ is the composition-dependent mismatch strain in the quantum dot, ϵ_m being the equi-biaxial mismatch strain arising due to the difference in the lattice constants between species A and B. In our calculations, the quantum dot and the substrate are assumed to be isotropic linear elastic materials with identical elastic constants, C_{ijkl}. For a given shape and size of the quantum dot, we have determined the equilibrium composition profiles by minimizing the sum of the chemical and elastic energies with respect to local composition $c(\mathbf{x})$ using a quadratic programming method [15]. The elastic fields in the quantum dot from variations in the local composition are computed using finite element methods. A combination of these techniques allows us to determine the equilibrium composition profiles for any shape, without invoking any approximations in computing the elastic fields.

The role of shape on the distribution of the alloy components is first considered for the case of cone-shaped quantum dots shown in Fig. 1(a). The composition profiles in these dots depend only on three parameters [14], namely, the average composition $\bar{c}$, the sidewall angle θ and the ratio of the chemical and elastic energy densities, $F_0 = F_m/(M\epsilon_m^2)$, where M is the biaxial modulus. This observation follows from the fact that the chemical and the elastic energies scale linearly with the volume of the quantum dot, which allows us to write their sum in the form

$$E_{ch} + E_{el} = M\epsilon_m^2 V_d\, \hat{W}(\bar{c}, \theta, F_0), \qquad (2)$$

where $\hat{W}$ is a dimensionless function. Since this function does not depend on size, the equilibrium composition profile in a "faceted" quantum dot with a given sidewall angle θ is independent of its volume, V_d.

The equilibrium composition profiles in 50-50 alloy quantum dots with sidewall angles of 15°and 45°are shown in Fig. 1(a). Here, we have taken $F_m = -0.2\, M\epsilon_m^2$, so that alloy thermodynamics favors complete mixing. However, strain leads to segregation of the larger alloy component (B) at the apex while the corners of the dot near the substrate are enriched in the other component (A). The degree of decomposition depends on the shape – segregation of the alloy components at the apex and at the periphery is much larger in the steeper dot. The 50% isocomposition profile in this case is located nearly half way between the substrate and the apex of the dot, while this profile in the shallower case lies between the axis of

	InGaAs/GaAs			SiGe/Si		
T	$M\epsilon_m^2$	F_m	$\Phi(30^\circ)$	$M\epsilon_m^2$	F_m	$\Phi(30^\circ)$
400 °C	4.86	-0.80	0.151	2.82	-3.00	0.021
600 °C	4.86	-1.91	0.075	2.82	-4.90	0.010

TABLE I: Segregation index for InGaAs/GaAs and SiGe/Si quantum dots with sidewall angles of 30°. The strain energy density, $M\epsilon_m^2$ and the coefficient of the mixing energy,[16] F_m are in given units of 10^8Joules/m^3. The degree of decomposition is considerably greater in InGaAs quantum dots compared to SiGe dots at typical growth temperatures.

symmetry and the periphery of the dot. Furthermore, the isocomposition profiles that lie above the substrate in the steeper dot develop a "cusp" at the axis of symmetry. This feature, which is absent in the shallower dot, should be observed by etching the structures with a selective chemical agent that removes material above a threshold level of composition. The 65% isocomposition surface profiles given in Fig. 1(b) for the two cases show very distinct shapes – the steeper dot develops a nearly flat top with a 'dimple' along its symmetry axis, whereas a deep pit is formed in the shallower dot. Similar features of etched surfaces have been observed in dome and pyramid shapes SiGe quantum dots, respectively [4–7]. However, kinetic effects, for example the smaller diffusion length of Ge compared to Si can also possibly give similar shapes upon selective etching [7]. Further experiments that consider the surface profiles as a function of annealing time are needed to determine if the measurements correspond to equilibrium predictions.

Strain-induced alloy segregation in the quantum dots can be analyzed in a quantitative manner by considering the segregation index Φ, which we define as:

$$\Phi(F_0,\theta) = \frac{4}{V_d}\int_{V_d} (c(\mathbf{x}) - \overline{c})^2\, dV\,. \qquad (3)$$

For a 50-50 alloy quantum dot, the alloy components

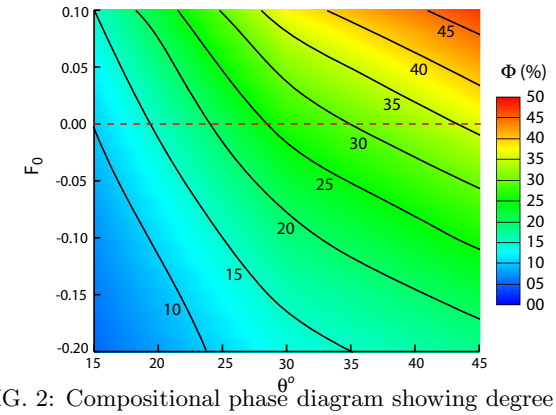

FIG. 2: Compositional phase diagram showing degree of segregation, Φ as a function of the parameter F_0 and the shape of the quantum dot represented by the angle of side-walls, θ. Even when the thermodynamic mixing energy favors mixing ($F_0 < 0$), the relaxation of strain for quantum dots with steep side-walls results in the alloy segregation within the quantum dot. Similarly, when thermodynamics favors phase separation ($F_0 > 0$), complete decomposition is not observed. The average composition of the quantum dot $\bar{c}$ is 0.5.

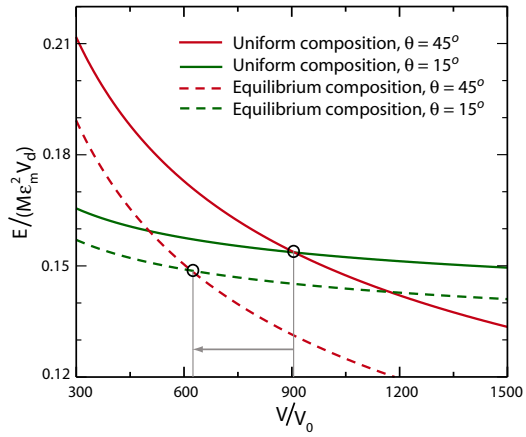

FIG. 3: Variation of the energy per unit volume for quantum dots with shallow and steep side-walls ($\theta = 15^\circ$and $\theta = 45^\circ$, respectively) as a function of their size (normalized by the characteristic volume, $V_0 = [\gamma/(M\epsilon_m^2)]^3$. The total energy of the decomposed dots (dotted lines) is lower than the energy of dots with uniform composition, $\overline{c} = 0.5$ (bold lines). However, the reduction in the energy is greater for the steeper dot, resulting in smaller critical size for transition in shape. The surface energies for shallow and steep side-walls are assumed to be identical and the mixing parameter $F_0 = -0.2$.

are completely mixed (i.e. $c(\mathbf{x}) = 0.5$ everywhere) when $\Phi = 0$, while $\Phi = 1$ corresponds to complete alloy decomposition. The computed level curves of the segregation index are plotted in Fig. 2 as a function of the ratio F_0 and the facet angle, θ and segregation indices for InGaS and SiGe quantum dots at typical growth temperatures are given in Table 1. As anticipated, the segregation index increases with increasing θ, but complete segregation of the alloy components is not achieved even when alloy thermodynamics favors phase separation ($F_0 > 0$). Similarly, complete mixing is only seen for very shallow dots when F_0 is sufficiently negative.

Next, we show that strain-induced segregation in quantum dots can substantially reduce the critical size for transition between the shapes with different facets. It is well known that with increasing size, shallow SiGe and InGaAs dots transform to steeper domes,[12, 13] as strain can be more efficiently relaxed in the latter case. The critical volume for shape transition depends on the surface energies of the facets and the nominally flat film, which, in general, can all be different from each other. However, the key features of this transition can be studied by assuming that all the surface energies involved are equal.[17] In this case, for dots with uniform composition, shape transitions occur at a size when the gain in the elastic energy obtained by the formation of the steeper dots offsets the cost of forming the sidewall surfaces. However, if the decomposition of the alloy is permitted, one can see that steeper dots allow for even larger reduction of the elastic energy as the alloy components can redistribute themselves more readily to strain-relaxed regions (Fig. 1). Using the dimensionless function $\hat{W}$ (Eq. 2) obtained from our optimization procedure, the total energy

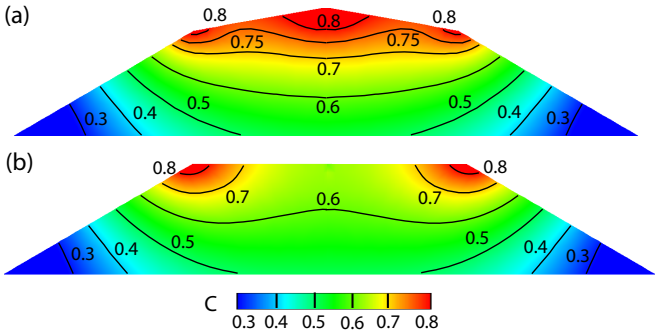

FIG. 4: Equilibrium composition profiles in axisymmetric quantum dots with (a) "dome" shape, the angles of the sidewalls being 30^o and 15^o, and (b) a truncated-cone shape with a sidewall angle of 30^o. While the composition profiles are similar near the base, larger strain relaxation in the regions near the corners results in a greater segregation in the apex of the dome-shaped quantum dot. The composition profiles are obtained for $F_0 = -0.2$ and $\bar{c} = 0.5$.

of an alloy dot can then be expressed as

$$E = M\epsilon_m^2 V_d \; \hat{W}(\overline{c}, \theta, F_0) + \gamma \, V_d^{2/3} \hat{\Gamma}(\theta)\,, \qquad (4)$$

where the surface energy, γ, is assumed to be independent of the facet angle, θ and $\hat{\Gamma}(\theta) = \pi^{1/3} 3^{2/3} (\tan\theta)^{-2/3} (\sqrt{1+\tan^2\theta} - 1)$. A plot of the energy per unit volume of decomposed dots in Fig. 3 (for $F_0 = -0.2$) shows that the volume to transition from a sidewall angle of 15° to 45° reduces by nearly 30% relative to the transformation volume of the to the dots with uniform composition.

In equilibrium, SiGe and InGaAs quantum dots can also adopt shapes that consists of two or more facet orientations [12, 13]. The computed equilibrium composition maps in such dome and truncated-pyramid shaped quantum dots are shown in Fig. 4. A distinguishing feature of these dots is the intricate pattern of isocomposition profiles that can be attributed to the presence of "corners" formed by the intersection of different facets. Since such corners allow for relaxation of mismatch strain, the free energy can be lowered by segregation of the larger alloy component in these regions. The number of extrema in the composition maps can therefore be directly correlated to the occurrences of facet intersections in the dot shape. The composition profiles in the regions close to the periphery of the base, however, are similar to the corresponding profiles in conical dots in Fig. 1. We have also studied composition profiles in Gaussian-shaped quantum dots [18] and found that the composition profiles are strongly influenced by the both the slopes and the curvatures of the surfaces.

In summary, we have developed an efficient method to compute composition maps in strained alloy quantum dots and have shown that the composition profiles depend strongly on the slopes and curvatures of the surfaces of the dots as well as the presence of other geometric features such as corners and edges. Our approach provides a means to rigorously study the interdependence of the shape, strain and composition in lattice mismatched systems. The method can therefore be employed to analyze compositional patterning in small scale structures such as nanowires,nanorings, nanotrees, quantum fortresses, quantum posts and quantum dot molecules. The research support of the NSF through the Brown University MRSEC program is gratefully acknowledged.

[1] J. Drucker, IEEE J. Quan. Elec. **38**, 975 (2002).
[2] J. Stangl, V. Holy and G. Bauer, Rev. Mod. Phys. **76**, 725 (2004).
[3] M. Floyd, Y. Zhang, K. P. Driver, J. Drucker, P.A. Crozier and D. J. Smith, Appl. Phys. Lett. **82**, 1473 (2003).
[4] A. Malachias, S. Kycia, G. Medeiros-Ribeiro, R. Magalhães-Paniago, T. I. Kamins and R. S. Williams, Phys. Rev. Lett. **91**, 176101 (2003).
[5] U. Denker, M. Stoffel and O. G. Schmidt, Phys. Rev. Lett. **90**, 196102 (2003).
[6] M. S. Leite, G. Medeiros-Ribeiro, T. I. Kamins and R. S. Williams, Phys. Rev. Lett. **98**, 165901 (2007).
[7] G. Katsaros, G. Costantini, M. Stoffel, R. Esteban, A. M. Bittner, A. Rastelli, U. Denker, O. G. Schmidt and K. Kern, Phys. Rev. B **72**, 195320 (2005).
[8] G. Medeiros-Ribeiro, and R. S. Williams, Nano Lett. **7**, 223 (2007).
[9] B. J. Spencer and M. Balanariu, Phys. Rev. Lett. **95**, 206101 (2005).
[10] N. Liu, J. Tersoff, O. Baklenov, A. L. Holmes and C. K. Shih Phys. Rev. Lett. **84**, 334 (2000).
[11] G. Hadjisavvas and P. C. Kelires, Phys. Rev. B **72**, 075334 (2005); C. Lang, D. J. H. Cockayne and D. Nguyen-Manh, Phys. Rev. B **72**, 155328 (2005).
[12] G. Medeiros-Ribeiro, M. Bratkovski, T. I. Kamins, D. A. A. Ohlberg and R. S. Williams, Science **279**, 353 (1998); F. M. Ross, R. M. Tromp and M. C. Reuter, Science **286**, 1931 (1999).
[13] G. Constantini, A. Rastelli, C. Manzano, P. Acosta-Diaz, G. Katsaros, R. Songmuang, O. G. Schmidt, H. Von Kanel and K. Kern, J. Crys. Growth **278**, 38 (2005).
[14] The contribution to the total energy of the quantum dot from the first term in $f(c)$ is $\Delta F(T)\bar{c}V_d$, where $\bar{c}$ is the average composition in the dot. If $\bar{c}$ is specified, this term is independent of the composition profile in the dot, $c(\mathbf{x})$ and therefore does not play a role in the determination of the equilibrium distribution of alloy components.
[15] K. Schittkowski, Ann. Op. Res. **5**, 485 (1985).
[16] The coefficient $F_m(T)$ is obtained by fitting $f(c)$ to the mixing energy density [9], $\Omega c(1-c) + (k_B T/v_a)\,[c\log c + (1-c)\log(1-c)]$, where the regular solution interaction parameter Ω is taken to be [9] 3.47 and 4.12 $\times 10^8$ Joules/m^3 for SiGe/Si and InGaAs/GaAs, respectively and v_a is the atomic volume.
[17] Transitions in the more general case with orientation dependent surface energies and the equilibrium shapes of dots with two or more facets (Figure 5) will be considered in a forthcoming publication.
[18] N. V. Medhekar et. al., (forthcoming).